Environ Res Tec, Vol. X, Issue. X, pp. 00–00, XXX,

Environmental Research and Technology
https://ert.yildiz.edu.tr - https://dergipark.org.tr/tr/pub/ert
DOI: https://10.35208/ert.1424621

Environmental Research & Technology

Research Article

Narrowing band gap of ZnO codoping (Al+Mn) as a photocatalyst candidate for degraded textile dye wastewater

Aprilion KRISANDI*[1], Heru HARSONO[1], Nurfina YUDASARI[2]

[1]Department of Physics, Brawijaya University, Jl. Kota Malang, Jawa Timur, Indonesia
[2]Research Center for Photonics – National Research and Innovation Agency, South Tangerang, Indonesia

ARTICLE INFO

Article history
Received: 23 January 2024
Revised: 31 May 2024
Accepted: 30 July 2024

Key words:
Gap energy; Photodegradation; Textile tye; ZnO

ABSTRACT

Photocatalyst degradation is one method to reduce industrial textile dye pollution in water. In this study, ZnO material was synthesized by codoping Al and Mn using the chemical coprecipitation method to determine the structural and optical properties of the material. This research found that the structure of ZnO after codoping Al and Mn did not change the hexagonal wurtzite phase but changed in other lattice parameters. The addition of Mn and Al codoping is reported to affect the intensity of XRD peaks, especially on the 101 lattice. The higher the scattering peak, the more angular the shift, indicating the magnitude of oxygen vacancies. The addition of Mn with 0% concentration shows the smallest lattice parameter among the other four samples. This indicates that the oxygen vacancy of the sample without Mn is more significant than that with codoping Mn. The reflectance measurement results show that the energy gap value of ZnO (Al+Mn), with a 0% Mn percentage, reaches an immense value, which is 3.290 eV. The smallest energy gap is ZnO (Al+Mn) with 4% codopping Mn which is 3.258 eV. With this consideration, ZnO (Al+Mn) with 0% Mn percentage is suitable to be applied as a Congo Red photodegradation agent, and ZnO (Al+Mn) with 4% codoping Mn is appropriate to be used as a Methylene Green photodegradation agent.

Cite this article as: Krisandi A, Harsono H, Yudasari N. Narrowing band gap of ZnO codoping (Al+Mn) as a photocatalyst candidate for degraded textile dye wastewater. Environ Res Tec 2024;7(4)00–00.

INTRODUCTION

The textile industry is increasing in all countries [1]. This is based on the fact that textiles are the primary needs of the people. Besides the magnitude of the textile industry, the negative impact on the environment produced is also significant. One of them is textile dye waste. Textile dye waste is an organic waste that is difficult to degrade. When this textile waste is disposed of in the river, it will cause water pollution [1–4]. Uncontrolled water pollution will affect the quality of water, the water ecosystem, and other problems. This problem needs to be solved in various ways. One uses photocatalysts to break down the bonds of textile dyes that have bonded with water molecules [3–5].

Textile dye waste that pollutes the environment will harm the environment and human health even in low concentrations. This happens because of the high composition of toxic textile dyes. In terms of the environment, this dye waste will increase Biochemical (BOD) and Chemical (COD) Oxygen Demand. This will directly inhibit further photosynthesis so aquatic plants will be disturbed. In addition, aquatic animals will stay away from the area because the aquatic environment is no longer healthy. Potential negative impacts also occur in humans. Like Azure B type textile dye waste, this type of dye waste has the potential to trigger gene mutation. This waste if contaminating the human body will be able to intercalate with the helical structure of DNA and RNA duplex [1]. Another potentially mutagenic dye is Disperse red.

***Corresponding author.**
*E-mail address: aprilionkris@student.ub.ac.id

The behavior of this mutagen can increase the frequency of micronuclei which is key for cancer characterization. Disperse Orange also shows a similar pattern. The behavior of mutagens that induce DNA damage can cause base shifts that alter the reading of the genetic code [3].

Removing dye sewage is an action that must be taken because of its serious effects on the sustainability of living things. Various ways are done to overcome this including Adsorption, coagulation, and filtering. However, these methods are costly and inefficient. One of the other methods offered is the photocatalyst method. This method involves semiconductor materials such as ZnO [4, 5]. ZnO semiconductor material is one of the photocatalysts that is being intensively developed. It has the advantages of being cheap, widely available, non-toxic, and easily modified [6–9]. These advantages are considered suitable to answer the problems of the textile industry, especially as a dye pollution degradation agent. ZnO reacted with dye waste liquid will respond if it gets energy from outside. The energy used is photon energy. This mechanism is referred to as a photocatalyst [10, 11]. Photons exposed to the ZnO solution with textile dyes will stimulate electrons to excite from the valence band to the conduction band. This mechanism will form reactive oxygen species that are useful as photodegradation agents [12–14].

Pure ZnO has a reasonably wide energy gap value of 3.37 eV and an excitonic binding energy of 60 meV [6, 15–17]. In this condition, the UV spectrum is needed to regenerate electron-hole recombination. ZnO structure modification is one way to narrow the energy gap value. However, the limitations of ZnO are limited conductivity and low charge concentration carrier ability. This causes the low-efficiency value of ZnO material. Therefore, it is necessary to modify the two factors mentioned. One strategy that can be done is to make structural modifications that can improve electron transport capabilities. Researchers have intensively added doping with metal ions. Some use group III metal dopping such as Al, In, Ga, etc [18]. Of the many types of group III metals, aluminum (Al) is the most widely used for dopping. Al is a dopant used to obtain n-type ZnO with high conductivity, crystal quality, and optical properties. Adding Al in ZnO can reduce the energy gap from 3.37 eV to 3.28 eV. This is essential information for synthesizing ZnO as a photocatalyst agent [16].

Modifying ZnO by adding Al doping has not significantly changed optical properties. The high doping concentration of up to 5% wt did not decrease the energy gap significantly [13, 15, 19–22]. This happens because the Oxygen Vacancy that occurs is still not optimal. Therefore, codoping methods are necessary. The candidates for the second element are transition metals such as (V, Fe, Co, Ni, Mn, etc) [9, 18, 23]. According to some research, Mn is one of the transition metals that can increase oxygen vacancy and absorb photon energy from the UV and visible ranges. However, dopping Mn with low concentrations <3% wt can reduce the energy gap value. Mn with concentrations >3% wt will increase the energy gap value with the presence of the second Mn phase [24–26].

Several methods for synthesizing ZnO with dopping include Coprecipitation, Sol-Gel, Hydrothermal, Chemical Vapor Deposition, Microemulsion Technique, Laser ablation, and Ball milling [27]. Each synthesis method has advantages and disadvantages. The physical technique can give maximum results, but the equipment setup is expensive; the chemical technique is more superficial and not so costly but has problems with reproducibility [28–30]. In this study, the synthesis technique used is co-precipitation, which is a bottom-up technique with a relatively simple and accessible tool setup. Codoping Al and Mn will synthesize ZnO material; Al concentration is fixed at 5% wt and Mn at 0% to 4% wt, respectively.

EXPERIMENTAL PROCEDURE

Material Synthesis

Zinc acetate (99.9%, Merck), Aluminum Chloride (99.9% Merck), Manganese Acetate (99.9% Merck), NaOH (97% Merck). All materials were prepared based on the concentration ratio of $Zn_{0.95-x}Al_{0.05}Mn_x$ with x = 0 to 0.04. The single Al-doped sample is referred to as 0% Mn, and the codoped sample is referred to as 1% Mn to 4% Mn. Each sample with a concentration of 1M was dissolved in 200 mL of deionized water and stirred using a magnetic stirrer at room temperature for 30 minutes. After mixing, the samples were allowed to stand for 30 minutes. After that, the sample solution was stirred again using a magnetic stirrer at a constant speed while the titration process was carried out using 1M NaOH solution. This titration process is carried out under room temperature conditions and continues to be carried out until it reaches a solution condition with a pH of 10. The titration process while stirring lasts for 90 minutes. After the solution has reached pH 10, the titration and stirring process is stopped. The beaker glass was closed using aluminum foil, and the sample was deposited overnight in room conditions. The precipitate was filtered using Whatman paper size 42 to separate the precipitate and liquid. This process was carried out by washing the sample using DI water and ethanol in a ratio of 3:1. After that, the sample was moved to the crucible and dried using an oven at 90 °C for 12 hours. This process aims to remove water and ethanol present in the sample. A temperature of 90 °C was chosen so that Al and Mn ions would not diffuse before calcination. After the samples were dried, they were pulverized using a mortar and calcined using a high furnace at 800 °C for 3 hours.

Characterization Procedure

The crystal structure of ZnO and its phase change were identified using X-ray diffraction (XRD) using a CuKα source (1.541862 Å). Crystal size was calculated using the Scherer equation

$$d = \frac{k\lambda}{\beta \cos\theta} \quad (1)$$

d is crystallite size, Lambda (λ) is the X-ray wavelength, Betha (β) is the FWHM in radians, Theta (θ) is the Bragg Angle and K is the Scherer constant 0.9.

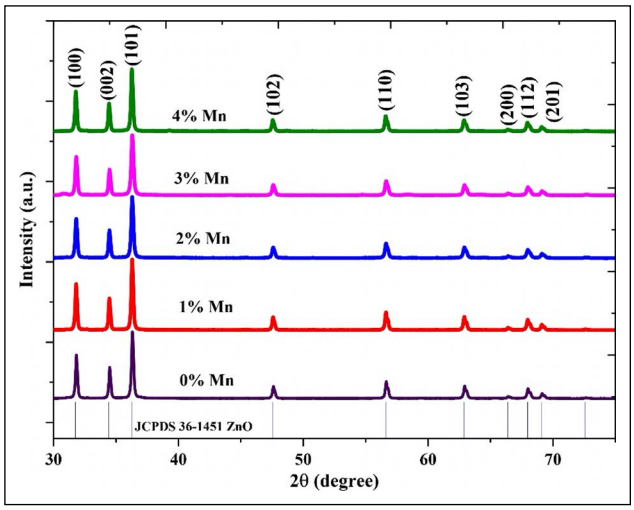

Figure 1. XRD spectra.

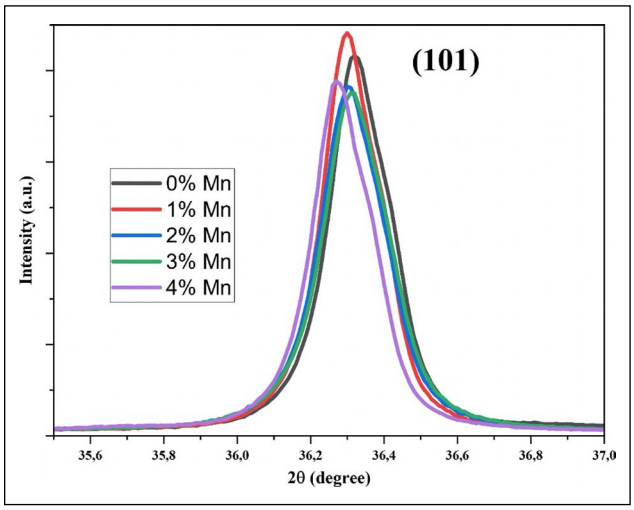

Figure 2. 101 peak shifting.

Table 1. The lattice parameter of pure ZnO and codopping ZnO

Mn concentration	2 Theta (degree) 101	Crystalline size D (nm)	d_{hkl}	Lattice parameter (Å)	
				a=b	c
Pure ZnO ref [31]	36.450	46.200	2.464	3.260	5.219
0%	36.330	39.767	2.471	2.853	5.198
1%	36.311	41.549	2.472	2.855	5.202
2%	36.313	37.736	2.472	2.854	5.201
3%	36.321	36.980	2.471	2.853	5.199
4%	36.285	40.955	2.473	2.856	5.205

Optical properties were observed using Ocean Optic reflectance spectroscopy with a wavelength range of 200–1110 nm radiation. Reflectance testing of the material was carried out to calculate the energy gap value of the material doped using Al and Mn. The optical band gap for codoping Al and Mn ZnO was measured using the following equation

$$(F(R)h\upsilon)^2=A(h\upsilon-E_g) \quad (2)$$

F(R) is an absorption value, A is a constant, hυ is the photon energy, and E_g is the energy gap of the material. The energy gap can be calculated by plotting a graph of $(F(R)hv)^2$ versus hυ. The extrapolation point of the linear part that meets the abscissa point will be given as the energy gap value of a material.

RESULT AND DISCUSSION

Structural Properties

Figure 1 shows the spectra of ZnO codoping Al and Mn with different concentrations (0, 1, 2, 3, 4 %wt). All XRD results show the hexagonal wurtzite phase form as in Pure ZnO. This is confirmed by overlaying the spectra on JCPDS data No. 36-1451, which matches the space group $P_{63}mc$. The spectra show that the structure of ZnO remains unchanged in single dopping of Al and codoping of Al, Mn, both at low to highest percentages, and the observed phase remains a Wurtzite structure. Figure 1, which shows the XRD pattern, shows no additional peaks. This means that the incorporation of Al^{3+} and Mn^{2+} ions substitute into interstitial sites or replace the presence of Zn^{2+} ions in the lattice without changing the wurtzite ZnO structure. In pure ZnO, Zn^{2+} ions have an ion radius of 0.74Å, smaller than Mn^{2+} ions of 0.80 Å, and larger than Al^{2+} ions of 0.53Å.

From the XRD pattern in Figure 1, grating 101 has the highest intensity of all gratings in all samples. Peak 101 is enlarged to see changes in the pattern of each sample. Figure 2 is a magnification of peak 101. There is a 1% to 4% peak shift pattern rather than 0% samples. This shift occurs because Mn^{2+} ions, which have a larger ion radius, replace Zn^{2+} ions in the crystal lattice. The presence of Al^{3+} ions also determines the peak height. The 1% Mn peak shows the highest position, which indicates that Al^{3+} ions are inserted more in place of Zn^{2+} than Mn^{2+}. This event occurs because the percentage of dopping in the sample is indeed more excellent Al with a ratio of Al % to Mn of 5%: 1%. However, as the percentage of Zn decreases and the rate of Mn increases, the peak also decreases until the Mn 4% condition changes to a non-linear pattern. This is indicated due to changes in the lattice parameters.

The lattice parameter values calculated using the equation written in Ravi Kant's [30] part of the data are presented in Table 1. The lattice value c looks smaller than the pure

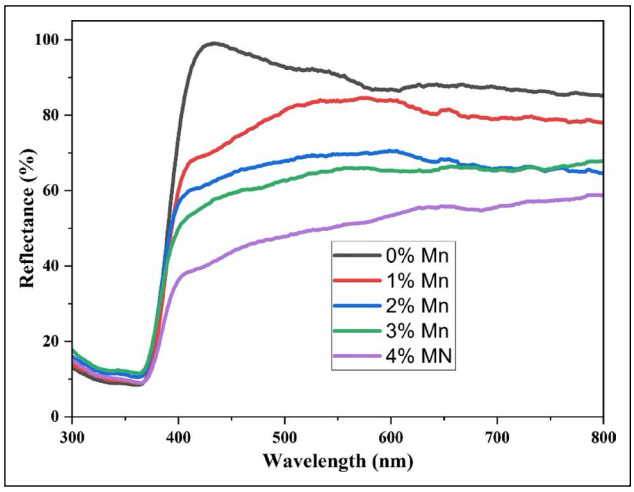

Figure 3. Reflectance graphic.

ZnO standard of 5.219 Å. This indicates the presence of oxygen vacancies in the material dropped by Al^{3+} and Mn^{2+} ions. The lattice parameter value does not show a value that continues to rise with the increase in Mn doping, but the lattice parameter value changes along with the doping ratio. For ZnO with a single Al dopping or Mn 0% sample, lattice parameters a and c values are the smallest compared to the other four samples. This may be due to the small dopant radius of Al^{3+} ions that replace Zn^{2+}. This also has an impact on the small lattice parameter values. However, when the percentage of Mn^{2+} dopping increases to the highest ratio of 4% Mn. The lattice parameter value reaches its highest value compared to the other four samples. This is probably because Mn^{2+} ions dominate in the replacement of Zn^{2+} ions. The lattice parameter value becomes larger since Mn^{2+} ions are more significant than Zn^{2+}. The size of the lattice parameter is substantial to discuss because it relates to the oxygen vacancy in the sample; the smaller the size of the lattice parameter, the more likely the presence of oxygen vacancy, which is helpful in the photodegradation process. ZnO (Al+Mn) with 0% Mn percentage shows the smallest lattice parameter. It indicates that this sample will produce more oxygen vacancy than others.

Optical Properties

Figure 3 represents the reflectance spectra of the Al and Mn codoping ZnO samples in the wavelength range of 300 to 800 nm. Uv-Vis spectroscopy is used to study the reflectance pattern of solid materials with a certain thickness. This helps scientists determine the energy gap value of the modified material, especially the effect of co-dopping ZnO (Al+Mn). Figure 4 shows the energy gap value of each of the characterized samples. The linear dependence between the value of $(F(R)hv)^2$ versus hν indicates that Al and Mn codoped ZnO is a semiconductor with a direct band gap. The direct band gap is calculated using the Kulbecka-Munk method in Equation 2.

The calculated band gap change values and comparison with the reference band gap are shown directly in Figure 4a. All band gap values of materials doped using Al and Mn are lower than that of pure ZnO. This decrease in band gap value, as shown in Figure 4b, is likely due to the incorporation of Al and Mn ions in the Zn lattice, which creates a new recombination pattern. This can be confirmed from the discussion of changes in the crystal structure of XRD results. As described by Gaurav Saxena [31], the decrease in energy gap value, along with the addition of Al and Mn doping, can be illustrated as a form of p-d spin exchange interaction between localized d electrons resulting from the substitution of Al^{3+} and Mn^{2+} ions. The sample with the largest percentage of Mn produces the most significant decrease in the energy gap. This is due to the solid p-d assimilation between O and Mn. So, adding Al and Mn co-dopping will reduce the energy gap value; this is in line with the initial purpose of the experiment, which is to reduce the energy gap of the material as a candidate for photocatalyst and pollutant removal applications.

Photodegradation Mechanism and its Relationship with the Energy Gap of the Material

The mechanism of photodegradation can be seen visually in Figure 5. What is modified is the value of Eg. The smaller the energy gap value, the easier for electrons to excite from VB (Valency Band) to CB (Conduction Band). The

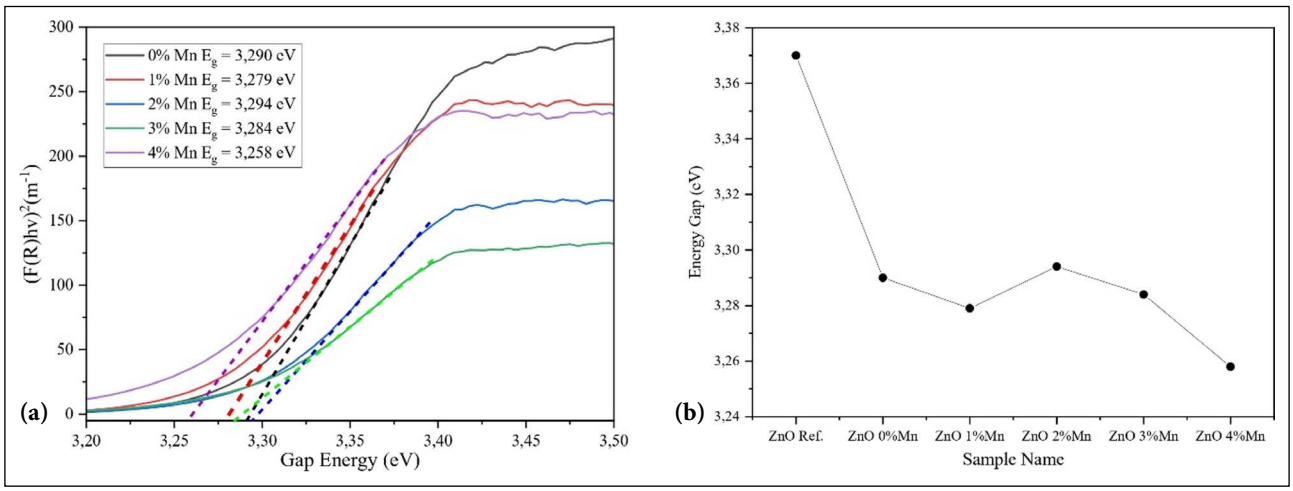

Figure 4. Band gap energy **(a)** Kubelcka Munk measurement **(b)** decreased energy gap value.

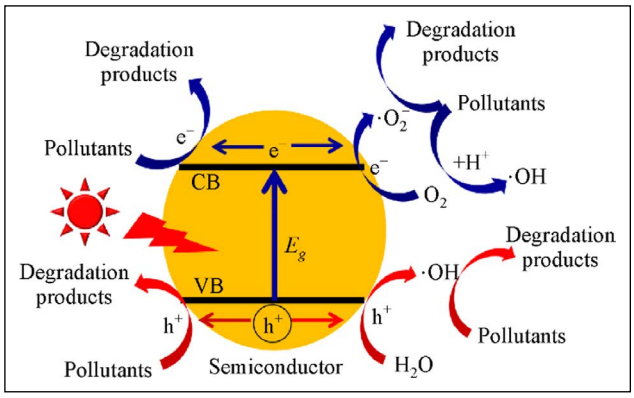

Figure 5. Photodegradation mechanism [33].

smaller the energy gap, the narrower the gap between the ribbons. The narrower the band gap, the easier for electrons to excite. If electrons are easily excited by small energy, the oxygen vacancies will get bigger. This will affect the formation of •O2⁻ (Oxygen Free Radicals), determining the photodegradation rate.

Various researchers have examined the photodegradation of textile dye effluents using ZnO materials. The photodegradation mechanism is that ZnO powder modified using codoping is dissolved in textile dye waste. Then, the mixture is irradiated using light in the UV-Vis range. However, UV irradiation is recommended for UV materials because it has a maximum energy value of 3–4 eV to reach the ZnO energy gap. This increases the possibility of expanding the photodegradation ability of the five modified ZnO (Al+Mn) samples with the highest Mn concentration of 4% Mn and the smallest gap energy value of 3.258 eV. Using a 4% Mn doping sample and comparing it with related research shown in Table 2, this modified sample can be a candidate for degrading Methylene Green textile dyes, as done by A. Mahesha [15] using ZnO doped with Cr^{3+} ions. This modification decreased the energy gap to 3.27 eV. Sample ZnO (Al+Mn) with 0% Mn, which has the most significant gap energy value (3.29 eV), also needs to be considered for use as a photodegradation agent. This is based on the high possibility of vacant oxygen due to the single doping of Al. The textile dye that this sample can degrade is Congo Red. According to Table 2, Congo Red requires a degradation agent with an energy gap of 3.3 eV, and this sample is suitable for degrading Congo Red.

CONCLUSION

ZnO material with fixed Al doping and Mn variation has been successfully made using a simple coprecipitation method. Various characterizations have ensured this newly modified material is suitable as a textile dye degradation agent candidate. The parameters used as a benchmark are structural and energy gap changes. Crystal structure observation was done using X-ray diffraction. From the reported discussion, it can be concluded that the single doping of ZnO with Al and codoping of ZnO with Al and Mn

Table 2. Reference data ZnO dopping as a dye photodegradation

No	Doppant %wt	Gap energy (eV)	Dye	Ref
1	Cr^{3+} 9%	3,27	MG	A Mahesha [15]
2	Co^{2+} 2%	3,06	MG	Al-Namshah [32]
3	Fe^{2+} Pure	2,97	MB	Sabrina [28]
4	Cu^{2+} 3%	3,19	MB IC	KV Karthik [33]
5	Cu^{2+} 5%	3,23	RhB	KV Karthik [33]
6	Pure Zn^{2+} Nps	3,30	CR	B C Nwaiwu [34]

MG: Methylene green; MB: Methylene blue; IC: Indigo carmine; RhB: Rhodamine B; CR: Congo red.

did not change the main crystal structure, which is still observed as Hexagonal Wurtzite. In diffraction peak 101, it is observed that the higher the percentage of dopping, the more the peak shifts towards the slight diffraction angle. This indicates that the presence of oxygen vacancies is more significant. This structural pattern is confirmed by reflectance characterization, which calculates the energy gap value. The higher the doping of Mn, the smaller the energy gap. However, this energy gap change does not occur linearly because an atomic insertion behavior has not been fully revealed. Modification of ZnO (Al+Mn) with a 4% Mn percentage produces the smallest energy gap of 3.258 eV and the highest energy gap reached by ZnO (Al+Mn) with a 4% Mn which is 3.290 eV. The type of textile dye that can be degraded with this modification is Methylene Green for (Al+Mn) with 4% Mn and Congo Red for (Al+Mn) with 0% Mn.

ACKNOWLEDGEMENTS

The authors express their gratitude and appreciation to the National Research and Innovation Agency, especially the Photonics Research Center, for providing a laboratory for characterization and the BARISTA program, which helps support this research.

DATA AVAILABILITY STATEMENT

The author confirm that the data that supports the findings of this study are available within the article. Raw data that support the finding of this study are available from the corresponding author, upon reasonable request.

CONFLICT OF INTEREST

The author declared no potential conflicts of interest with respect to the research, authorship, and/or publication of this article.

USE OF AI FOR WRITING ASSISTANCE

Not declared.

ETHICS

There are no ethical issues with the publication of this manuscript.

REFERENCES

[1] B. Lellis, C. Z. Fávaro-Polonio, J. A. Pamphile, and J. C. Polonio, "Effects of textile dyes on health and the environment and bioremediation potential of living organisms," Biotechnology Research and Innovation, Vol. 3(2), pp. 275–290, 2019. [CrossRef]

[2] A. Rasool, S. Kiran, T. Gulzar, S. Abrar, A. Ghaffar, M. Sahid, S. Nosheen, and A. Naz, "Biogenic synthesis and characterization of ZnO nanoparticles for degradation of synthetic dyes: A sustainable environmental cleaner approach," Journal of Cleaner Production, Vol. 398, Article 136616, 2023. [CrossRef]

[3] L. D. Ardila-Leal, R. A. Poutou-Piñales, A. M. Pedroza-Rodríguez, and B. E. Quevedo-Hidalgo, "A brief history of color, the environmental impact of synthetic dyes and removal by using laccases," Molecules, Vol. 26(13) Article 3813. [CrossRef]

[4] M. F. Lanjwani, M. Tuzen, M. Y. Khuhawar, and T. A. Saleh, "Trends in photocatalytic degradation of organic dye pollutants using nanoparticles: A review," Inorganic Chemistry Communications, Vol. 159, Article 111613, 2024. [CrossRef]

[5] M. Lal, P. Sharma, L. Singh, and C. Ram, "Photocatalytic degradation of hazardous Rhodamine B dye using sol-gel mediated ultrasonic hydrothermal synthesized of ZnO nanoparticles," Results in Engineering, Vol. 17, Article 100890, 2023. [CrossRef]

[6] F. Maldonado, and A. Stashans, "Al-doped ZnO: Electronic, electrical and structural properties," Journal of Physics and Chemistry of Solids, Vol. 71(5), pp. 784–787, 2010. [CrossRef]

[7] R. Anugrahwidya, N. Yudasari, and D. Tahir, "Optical and structural investigation of synthesis ZnO/Ag Nanoparticles prepared by laser ablation in liquid," Materials Science in Semiconductor Processing, Vol. 105, Article 104712, 2020. [CrossRef]

[8] N. Yudasari, A. Hardiansyah, Y. Herbani, M. M. S uliyanti, and D. Djuhana, "Single-step laser ablation synthesis of ZnO-Ag nanocomposites for broad-spectrum dye photodegradation and antibacterial photoinactivation," https://ssrn.com/abstract=4352158 Accessed on Sep 29, 2024. [CrossRef]

[9] C. Oeurn Chey, "Synthesis of ZnO and Transition Metals Doped ZnO Nanostructures, their Characterization and Sensing Applications," Linköping University Electronic Press, 2015. [CrossRef]

[10] W. S. Koe, J. W. Lee, W. C. Chong, Y. L. Pang, and L. C. Sim, "An overview of photocatalytic degradation: photocatalysts, mechanisms, and development of photocatalytic membrane," Environmental Science and Pollution Research, Vol. 27(3), pp. 2522–2565, 2020. [CrossRef]

[11] H. Fatima, "Western Australian School of Mines: Minerals, Energy and Chemical Engineering Synthesis and characterization of ZnO-based/derived nanoparticles as promising photocatalysts," Kappa Journal, Vol. 8(2), pp. 255–261, 2022.

[12] D. Blažeka, J. Car, N. Klobucar, A. Jurov, J. Zavasnik, A. Jagodar, E. Kovacevic, and N. Krstulovic, "Photodegradation of methylene blue and rhodamine b using laser-synthesized ZnO nanoparticles," Materials, Vol. 13(19), pp. 1–15, 2020. [CrossRef]

[13] R. Ghorbali, G. Esalah, A. Ghoudi, H. Guermazi, S. Guermazi, A. El Hdiy, H. Banhayoune, B. Duponchel, A. Oueslati, and G. Leroy, "The effect of (In, Cu) doping and co-doping on physical properties and organic pollutant photodegradation efficiency of ZnO nanoparticles for wastewater remediation," Ceramics International, Vol. 49(21), pp. 33828–33841, 2023. [CrossRef]

[14] R. E. Adam, G. Pozina, M. Willander, and O. Nur, "Synthesis of ZnO nanoparticles by co-precipitation method for solar-driven photodegradation of Congo red dye at different pH," Photonics Nanostruct, Vol. 32, pp. 11–18, 2018. [CrossRef]

[15] A. Mahesha, M. Nagaraja, A. Madhu, N. Suriyamurthy, S. Satyanarayana Reddy, M. Al-Dossari, N.S. Abd EL-Gawaad, S.O. Manjunatha, K. Gurushantha, and N. Srinatha, "Chromium-doped ZnO nanoparticles synthesized via auto-combustion: Evaluation of concentration-dependent structural, band gap-narrowing effect, luminescence properties and photocatalytic activity," Ceramics International, Vol. 4914, pp. 22890–22901, 2023. [CrossRef]

[16] D. Savitha, H. K. E. Latha, H. S. Lalithamba, S. Mala, and Y. Vasudev Jeppu, "Structural, optical and electrical properties of undoped and doped (Al, Al + Mn) ZnO nanoparticles synthesized by green combustion method using Terminalia catappa seed extract," Materials Today: Proceedings, Vol. 60, pp. 988–997, 2022. [CrossRef]

[17] A. M. Alsaad, Q. M. Al-Bataineh, A. A. Ahmad, Z. Albataineh, and A. Telfah, "Optical band gap and refractive index dispersion parameters of boron-doped ZnO thin films: A novel derived mathematical model from the experimental transmission spectra," Optik (Stuttg), Vol. 211, Article 164641, 2020. [CrossRef]

[18] M. A. Nawaz and P. Dissertation, "Effect of Transition Metals Doping on the Properties of ZnO Thin Films," [Master thesis], The Islamia University of Bahawalpur, 2016.

[19] P. Norouzzadeh, K. Mabhouti, M. M. Golzan, and R. Naderali, "Investigation of structural, morphological and optical characteristics of Mn substituted Al-doped ZnO NPs: A Urbach energy and Kramers-Kronig study," Optik (Stuttgart), Vol. 204, Article 164227, 2020. [CrossRef]

[20] A. Ashwini, L. Saravanan, V. Sabari, M. Astalakshmi, and N. Kanagathara, "Effect of Cu doping with varying pH on photocatalytic activity of ZnO nanoparticles for the removal of organic pollutants," Inorg Chemical Communications, Vol. 155, Article 111137, 2023. [CrossRef]

[21] A. Henni, A. Merrouche, L. Telli, and A. Karar, "Studies on the structural, morphological, optical and electrical properties of Al-doped ZnO nanorods prepared by electrochemical deposition," Journal of Electroanalytical Chemistry, Vol. 763, pp. 149–154, 2016. [CrossRef]

[22] R. C. Tiwari, "Structural, Optical and Electronic Properties of Zno Nanoparticles," [Master thesis], The University of Tulsa, 2017.

[23] A. Ciechan, and P. Bogusławski, "Theory of the sp–d coupling of transition metal impurities with free carriers in ZnO," Scientific Report, Vol. 11(1), Article 3848, 2021, [CrossRef]

[24] J. Gupta, P. A. Hassan, and K. C. Barick, "Structural, photoluminescence and photocatalytic properties of Mn and Eu co-doped ZnO nanoparticles," in Materials Today: Proceedings, Vol. 42, pp. 926–931, 2020. [CrossRef]

[25] R. Asih, R.M. Dhari, M. Baqiya, and F. Astuti, "Effects of Mn substitution on magnetic properties of ZnO nanoparticles," Key Engineering Materials, Vol. 855, pp. 166–171, 2020. [CrossRef]

[26] E. A. Batista, A. C. A. Silva, T. K. de Lima, E. V. Guimarães, R. S. da Silva, and N. O. Dantas, "Effect of the location of Mn2+ ions in the optical and magnetic properties of ZnO nanocrystals," Journal of Alloys and Compounds, Vol. 850, Article 156611, 2021. [CrossRef]

[27] N. H. Nam, and N. H. Luong, "Nanoparticles: Synthesis and applications," In: V. Grumezescu, and A. M. Grumezescu, (Eds.), Materials for Biomedical Engineering: Inorganic Micro- and Nanostructures, (pp. 211–240), Elseiver, 2019. [CrossRef]

[28] S. Roguai and A. Djelloul, "Structural, microstructural and photocatalytic degradation of methylene blue of zinc oxide and Fe-doped ZnO nanoparticles prepared by simple coprecipitation method," Solid State Communications, Vol. 334–335, Article 114362, 2021. [CrossRef]

[29] M. Hou, and J. Ge, "Armoring enzymes by metal-organic frameworks by the coprecipitation method," Methods in Enzymology, Vol. 590, pp. 59–75, 2017. [CrossRef]

[30] R. Kant, R. Singh, A. Bansal, and A. Kumar, "Effect of Mn-adding on microstructure, optical and dielectric properties Zn0.95Al0.05O nanoparticles," Physica E: Low-dimensional systems and Nanostructures, Vol. 131, Article 114726, 2021. [CrossRef]

[31] G. Saxena, I. A. Salmani, M. S. Khan, and M. S. Khan, "Structural co-related optical properties of Al and Cu co-doped ZnO nanoparticles," Nano-Structures and Nano-Objects, Vol. 35, Article 100986, 2023. [CrossRef]

[32] K. S. Al-Namshah, M. Shkir, F. A. Ibrahim, and M. S. Hamdy, "Auto combustion synthesis and characterization of Co-doped ZnO nanoparticles with boosted photocatalytic performance," Physica B: Condensed Matter, Vol. 625, Article 413459, 2022. [CrossRef]

[33] K. V. Karthik, A.V. Raghu, K.R. Reddy, R. Ravishankar, M. Sangeeta, N.P. Shetti, and C, V. Reddy, "Green synthesis of Cu-doped ZnO nanoparticles and its application for the photocatalytic degradation of hazardous organic pollutants," Chemosphere, Vol. 287, Article 132081, 2022. [CrossRef]

[34] B. C. Nwaiwu, E. E. Oguzie, and C. C. Ejiogu, "Photocatalytic degradation of Congo red using doped zinc oxide nanoparticles," EQA-International Journal of Environmental Quality, Vol. 60, pp. 18–26, 2024